Increased shear in the North Atlantic upper-level jet stream over the past four decades

Article

Accepted Version

Increased shear in the North Atlantic upper-level jet stream over the past four decades

Simon H. Lee, Paul D. Williams, and Thomas H. A. Frame

Department of Meteorology, University of Reading, Reading, U.K.

Earth's equator-to-pole temperature gradient drives westerly mid-latitude jet streams through thermal wind balance[1]. In the upper atmosphere, anthropogenic climate change is strengthening this meridional temperature gradient by cooling the polar lower stratosphere[2,3] and warming the tropical upper troposphere[4–6], acting to strengthen the upper-level jet stream[7]. In contrast, in the lower atmosphere, Arctic amplification of global warming is weakening the meridional temperature gradient[8–10], acting to weaken the upper-level jet stream. Therefore, trends in the speed of the upper-level jet stream[11–13] represent a closely balanced tug-of-war between two competing effects at different altitudes[14]. It is possible to isolate one of the competing effects by analysing the vertical shear instead of the speed, but this approach has not previously been taken. Here we show that, while the zonal wind speed in the North Atlantic polar jet stream at 250 hPa has not significantly changed since the start of the observational satellite era in 1979, the vertical shear has increased by 15% (with a range of 11–17%) according to three different reanalysis datasets[15–17]. We further show that this trend is attributable to the thermal wind response to the enhanced upper-level meridional temperature gradient. Our results indicate that climate change is having a larger impact on the North Atlantic jet stream than previously thought. The increased vertical shear is consistent with the intensification of shear-driven clear-air turbulence expected from climate change[18–20], which will affect aviation in the busy transatlantic flight corridor. We conclude that the impacts of climate change and variability on the upper-level jet stream are being partly obscured by the traditional focus on speed rather than shear.

In the northern and southern hemispheres, the mid-latitude baroclinic zone of the atmosphere is associated with a planetary-scale meridional temperature gradient between the equator and the pole. This temperature gradient generates westerly winds that strengthen with height – vertical wind shear – as a consequence of thermal wind balance[1]. Using pressure as a vertical coordinate, the vertical shear in the zonal wind, $-\partial u/\partial p$, is related to the meridional temperature gradient, $\partial T/\partial y$, by the thermal wind balance equation:

$$-\frac{\partial u}{\partial p} = -\frac{R}{fp}\frac{\partial T}{\partial y}\,, \tag{1}$$

where R is the specific gas constant for dry air, f is the Coriolis parameter, p is pressure, and y is northward distance. Aloft, the strong westerly winds generated by thermal wind balance form the polar (or mid-latitude) jet stream, the speed of which is typically maximised near the tropopause, where the sign of the meridional temperature gradient (and thus the sign of the vertical shear) reverses. The polar jet stream is often described as eddy-driven, because eddies are required to support non-zero surface westerlies. It is distinct from the subtropical jet stream, which is primarily caused by poleward transport of angular momentum in the Hadley cell[21]. The polar jet stream influences mid-latitude weather systems, with the storm tracks being essentially a surface expression of the jet stream[22]. It also plays an important role in commercial aircraft operations, partly because it creates strong headwinds and tailwinds on busy mid-latitude flight routes[23], but also because clear-air turbulence is generated by the associated intense vertical wind shear.

The mid-latitude meridional temperature gradients are being modified by anthropogenic climate change[24], and the jet streams are expected to adjust in response[23–25]. In the lower troposphere of the northern hemisphere, Arctic amplification caused primarily by lapse-rate feedbacks[26] is weakening the meridional temperature gradient and polar jet stream[8–10]. In contrast, in the upper troposphere and lower stratosphere, the meridional temperature gradient

is strengthening because of the combined effects of polar lower-stratospheric cooling and tropical upper-tropospheric warming, the latter caused by water vapour feedbacks releasing additional latent heat and reducing the lapse rate[7]. The vertically integrated thermal wind response is a tug-of-war between these two competing effects, with Arctic amplification acting to decrease the wind speed in the upper troposphere and lower stratosphere, but polar lower-stratospheric cooling and tropical upper-tropospheric warming acting to increase it. These competing influences suggest that upper-level trends in the jet stream may be better discerned through changes in vertical wind shear rather than absolute wind speed.

Here we analyse historic trends in the upper-level vertical wind shear over the North Atlantic. In future climate projections, the prevalence of clear-air turbulence at typical aircraft cruising altitudes increases more here than anywhere else globally[20]. We use data from the ERA-Interim reanalysis at 0.75° horizontal resolution[16], the NCEP/NCAR reanalysis at 2.5° horizontal resolution[15], and the JRA-55 reanalysis at 1.25° horizontal resolution[17]. The use of three independently produced reanalysis datasets allows us to quantify the sensitivity of our results to uncertainties in the state of the atmosphere. We take six-hourly data from the years 1979–2017 inclusive. We restrict the temporal coverage to the satellite era, because the sparsity of upper-level wind observations over the North Atlantic before 1979 substantially increases uncertainty in reanalysis datasets[27]. We consider data within the region defined by 30–70°N and 10–80°W. This latitudinal range is chosen to include the polar jet stream (and the busy transatlantic flight corridor) whilst excluding the subtropical jet stream. We focus on the shear at a pressure altitude of 250 hPa, corresponding to the climatological core of the polar jet stream, and equating to a typical aircraft cruising altitude of around 34,000 feet.

We begin by analysing annual-mean upper-level temperature trends. As shown in **Figure 1**, all three reanalysis datasets indicate a strengthening of the mid-latitude meridional temperature gradient at 250 hPa. The 250 hPa pressure surface evidently intersects the

tropopause at around 50–60°N, with lower-stratospheric cooling on the poleward side and upper-tropospheric warming on the equatorward side. The upper-tropospheric warming trend is slightly stronger in ERA-Interim and JRA-55, and the lower-stratospheric cooling trend is slightly stronger in NCEP/NCAR. Despite these minor differences, the spatial patterns and magnitudes of the temperature trends are broadly consistent across the datasets. Unlike the warming trends, the cooling trends are generally not statistically significant (except near Iceland in NCEP/NCAR), probably because of large inter-annual variability associated with the northern hemispheric circumpolar vortex[28].

To assess the vertical structure of the trends in the meridional temperature gradient, we calculate a bulk north–south temperature difference across the North Atlantic using a two-box method. On each pressure surface, annual-mean temperatures are averaged within a polar box (50–70°N, 10–80°W) and then subtracted from those averaged within a subtropical box (30–50°N, 10–80°W). This calculation yields a zonal-mean bulk meridional temperature difference, and the trends in this quantity are shown in **Figure 2**. There is good agreement between the reanalysis datasets, with all three showing a significant weakening of the meridional temperature gradient in the lower atmosphere and a significant strengthening in the upper atmosphere. There is a transition between these two influences at around 450 hPa. There are some minor discrepancies, with NCEP/NCAR showing both a faster weakening of the meridional temperature gradient in the lower atmosphere and a faster strengthening aloft. At 250 hPa, however, all three reanalysis datasets show a significant strengthening of the temperature difference by nearly 0.2 K decade^{-1}, consistent with **Figure 1**.

To assess the impacts of the increasing meridional temperature gradient at 250 hPa on the atmospheric circulation, time series of the annual-mean vertical shear in zonal wind, averaged over the region 30–70°N and 10–80°W, are shown in **Figure 3 (a).** All three reanalysis datasets are clearly in good agreement with respect to the inter-annual variability and the

superimposed upward trend. The multi-reanalysis ensemble-mean vertical wind shear shows a significant (p = 0.03) increase of 15% (0.07 m s^{-1} (100 hPa)$^{-1}$ decade^{-1}) over the 39-year period. The individual increases range from 11% in JRA-55 (0.06 m s^{-1} (100 hPa)$^{-1}$ decade^{-1}, p = 0.09) to 17% in ERA-Interim (0.08 m s^{-1} (100 hPa)$^{-1}$ decade^{-1}, p = 0.02) and 17% in NCEP/NCAR (0.08 m s^{-1} (100 hPa)$^{-1}$ decade^{-1}, p = 0.01). In contrast, as shown in **Figure 3 (b),** the annual-mean zonal wind speed averaged over the same region at 250 hPa has not significantly changed in any of the three datasets (p = 0.72 for the slope of the ensemble-mean trend). It is notable that there is less spread between the three datasets for the shear than the speed, possibly because the speed is biased low in NCEP/NCAR because of the relatively coarse resolution compared to ERA-Interim and JRA-55, whereas this bias evidently disappears when vertical differences are taken to compute the shear.

The increased shear without increased speed shown for the upper atmosphere in **Figure 3** indicates that the weaker meridional temperature gradient (and weaker vertical wind shear) in the lower troposphere is masking the stronger meridional temperature gradient (and stronger vertical wind shear) in the upper troposphere and lower stratosphere, through a large degree of cancellation in the vertically integrated thermal wind. We illustrate this effect by showing vertical profiles of trends in shear and speed throughout the depth of the troposphere in **Extended Data Figure 1.** The shear is strengthening within the jet core as well as throughout the broader region influenced by the jet stream (**Extended Data Figure 2**) and the trends are not attributable to a shift in the annual-mean latitude of the jet core (**Extended Data Figure 3**).

To relate trends in the meridional temperature gradient to trends in the vertical shear, we invoke the time derivative of the thermal wind balance equation (1):

$$-\frac{\partial}{\partial t}\frac{\partial u}{\partial p} = -\frac{R}{fp}\frac{\partial}{\partial t}\frac{\partial T}{\partial y} \; . \qquad (2)$$

We calculate both sides of this equation independently at each grid-point, as a measure of the extent to which the vertical wind shear changes are attributable to the local thermal wind response to the meridional temperature gradient changes. The time derivatives are evaluated as the linear trends over the period 1979–2017, calculated by applying ordinary least-squares regression to annual-mean values of $\partial u/\partial p$ and $\partial T/\partial y$ at each grid-point on the 250 hPa pressure surface. Maps of the left side of equation (2) – the directly calculated vertical wind shear trend, produced by differencing the wind fields at the two adjacent pressure levels – are shown in **Figure 4 (a, b, c)**. Maps of the right side of equation (2) – the expected vertical wind shear trend, produced by using the temperature field and assuming thermal wind balance – are shown in **Figure 4 (d, e, f)**. There is a clear trend towards stronger vertical shear at 250 hPa over almost the entire North Atlantic domain in all three reanalysis datasets. The trend is statistically significant in the core of the climatological jet stream and on the poleward flank. We note the similarity in spatial patterns between these observed vertical wind shear increases and future projections of increased clear-air turbulence[18,19]. The good agreement between the left and right sides of equation (2), in terms of both the spatial patterns (the pattern correlation coefficients are $r > 0.70$ in all three datasets) and magnitudes, confirms that the vertical wind shear trends are indeed largely attributable to the response of the thermal wind to the meridional temperature gradient trends. The small discrepancies are presumably attributable to the numerical finite differences used to estimate the derivatives, as well as to weak ageostrophic and non-hydrostatic effects.

In summary, we have identified the first observationally based evidence of increased vertical wind shear in the North Atlantic upper-level jet stream over the satellite era (1979–2017). The increase of 15% (with a range of 11–17%) is statistically significant, is present in three independently produced reanalysis datasets, and is attributable to the thermal wind response to the strengthening upper-level meridional temperature gradient. The stronger shear is

consistent with the intensification of clear-air turbulence expected from climate change[18–20], because clear-air turbulence is generated by strong vertical wind shear (which means small Richardson number; we note that a 15% shear increase implies roughly a 30% Richardson number decrease, because of their inverse square relationship). In contrast to the large increase in vertical wind shear, we find that the zonal wind speed has not significantly changed, consistent with previous studies[11,12]. The explanation for this effect is that, in the vertically integrated thermal wind balance equation, the weaker meridional temperature gradient and weaker vertical wind shear in the lower troposphere are mostly offsetting the stronger meridional temperature gradient and stronger vertical wind shear aloft. Increased vertical wind shear has important implications, not only for clear-air turbulence and its impacts on aviation, but also for the turbulent mixing of atmospheric constituents across the tropopause[29], with potentially significant consequences for large-scale atmospheric thermodynamics and dynamics[30].

Our results indicate that climate change is having a larger impact on the North Atlantic jet stream than previously thought. We conclude that the impacts of climate change and variability on the upper-level jet stream are being partly obscured by the traditional focus on speed rather than shear. We suggest that climate-modelling studies into the response of the jet streams to climate change should therefore include consideration of the vertical shear as well as the speed. We anticipate that inter-model differences in upper-level vertical wind shear trends will have a clear interpretation in terms of different upper-level temperature trends. On the other hand, inter-model differences in upper-level wind speed trends may be more difficult to interpret, because of different balances in the competition between temperature trends at upper and lower levels.

References

1. Wallace, J. M. & Hobbs, P. V. *Atmospheric Science: An Introductory Survey*. (Academic Press, 2006).

2. Held, I. M. Large-Scale Dynamics and Global Warming. *Bull. Am. Meteorol. Soc.* **74**, 228–241 (1993).

3. Thompson, D. W. J. & Solomon, S. Recent stratospheric climate trends as evidenced in radiosonde data: Global structure and tropospheric linkages. *J. Clim.* **18**, 4785–4795 (2005).

4. Allen, R. J. & Sherwood, S. C. Warming maximum in the tropical upper troposphere deduced from thermal winds. *Nat. Geosci.* **1**, 399–403 (2008).

5. Mitchell, D. M., Thorne, P. W., Stott, P. A. & Gray, L. J. Revisiting the controversial issue of tropical tropospheric temperature trends. *Geophys. Res. Lett.* **40**, 2801–2806 (2013).

6. Sherwood, S. C. & Nishant, N. Atmospheric changes through 2012 as shown by iteratively homogenized radiosonde temperature and wind data (IUKv2). *Environ. Res. Lett.* **10**, 054007 (2015).

7. Lorenz, D. J. & DeWeaver, E. T. Tropopause height and zonal wind response to global warming in the IPCC scenario integrations. *J. Geophys. Res. Atmos.* **112**, 1–11 (2007).

8. Francis, J. A. & Vavrus, S. J. Evidence linking Arctic amplification to extreme weather in mid-latitudes. *Geophys. Res. Lett.* **39**, 1–6 (2012).

9. Haarsma, R. J., Selten, F. & van Oldenborgh, G. J. Anthropogenic changes of the thermal and zonal flow structure over Western Europe and Eastern North Atlantic in CMIP3 and CMIP5 models. *Clim. Dyn.* **41**, 2577–2588 (2013).

10. Francis, J. A. & Vavrus, S. J. Evidence for a wavier jet stream in response to rapid

Arctic warming. *Environ. Res. Lett.* **10**, 014005 (2015).

11. Archer, C. L. & Caldeira, K. Historical trends in the jet streams. *Geophys. Res. Lett.* **35**, 1–6 (2008).

12. Pena-Ortiz, C., Gallego, D., Ribera, P., Ordonez, P. & Del Carmen Alvarez-Castro, M. Observed trends in the global jet stream characteristics during the second half of the 20th century. *J. Geophys. Res. Atmos.* **118**, 2702–2713 (2013).

13. Manney, G. L. & Hegglin, M. I. Seasonal and Regional Variations of Long-Term Changes in Upper-Tropospheric Jets from Reanalyses. *J. Clim.* **31**, 423–448 (2018).

14. Francis, J. A. Why are Arctic linkages to extreme weather still up in the air? *Bull. Am. Meteorol. Soc.* **98**, 2551–2558 (2017).

15. Kalnay, E. *et al.* The NCEP/NCAR 40-year reanalysis project. *Bull. Am. Meteorol. Soc.* **77**, 437–471 (1996).

16. Dee, D. P. *et al.* The ERA-Interim reanalysis: Configuration and performance of the data assimilation system. *Q. J. R. Meteorol. Soc.* **137**, 553–597 (2011).

17. Kobayashi, S. *et al.* The JRA-55 Reanalysis: General Specifications and Basic Characteristics. *J. Meteorol. Soc. Japan. Ser. II* **93**, 5–48 (2015).

18. Williams, P. D. & Joshi, M. M. Intensification of winter transatlantic aviation turbulence in response to climate change. *Nat. Clim. Chang.* **3**, 644–648 (2013).

19. Williams, P. D. Increased light, moderate, and severe clear-air turbulence in response to climate change. *Adv. Atmos. Sci.* **34**, 576–586 (2017).

20. Storer, L. N., Williams, P. D. & Joshi, M. M. Global Response of Clear-Air Turbulence to Climate Change. *Geophys. Res. Lett.* **44**, 9976–9984 (2017).

21. Lee, S. & Kim, H. The Dynamical Relationship between Subtropical and Eddy-Driven Jets. *J. Atmos. Sci.* **60**, 1490–1503 (2003).

22. Hannachi, A., Woollings, T. & Fraedrich, K. The North Atlantic jet stream: A look at preferred positions, paths and transitions. *Q. J. R. Meteorol. Soc.* **138**, 862–877 (2012).

23. Williams, P. D. Transatlantic flight times and climate change. *Environ. Res. Lett.* **11**, 024008 (2016).

24. Vallis, G. K., Zurita-Gotor, P., Cairns, C. & Kidston, J. Response of the large-scale structure of the atmosphere to global warming. *Q. J. R. Meteorol. Soc.* **141**, 1479–1501 (2015).

25. Woollings, T. & Blackburn, M. The North Atlantic jet stream under climate change and its relation to the NAO and EA patterns. *J. Clim.* **25**, 886–902 (2012).

26. Stuecker, M. F., Bitz, C. M., Armour, K. C., Proistosescu, C. & Kang, S. M. Polar amplification dominated by local forcing and feedbacks. *Nat. Clim. Chang.* **8**, 1076–1081 (2018).

27. Fujiwara, M. *et al.* Introduction to the SPARC Reanalysis Intercomparison Project (S-RIP) and overview of the reanalysis systems. *Atmos. Chem. Phys.* **17**, 1417–1452 (2017).

28. Waugh, D. W., Sobel, A. H. & Polvani, L. M. What is the polar vortex and how does it influence weather? *Bull. Am. Meteorol. Soc.* **98**, 37–44 (2017).

29. Shapiro, M. A. Turbulent Mixing within Tropopause Folds as a Mechanism for the Exchange of Chemical Constituents between the Stratosphere and Troposphere. *J. Atmos. Sci.* **37**, 994–1004 (1980).

30. Maycock, A. C., Joshi, M. M., Shine, K. P. & Scaife, A. A. The circulation response to

idealized changes in stratospheric water vapor. *J. Clim.* **26**, 545–561 (2013).

Acknowledgements

S.H.L. acknowledges support through a Ph.D. studentship from the Natural Environment Research Council SCENARIO Doctoral Training Partnership (reference NE/L002566/1).

Author contributions

S.H.L. and P.D.W. jointly conceived the study. S.H.L. performed the data analysis and produced the figures with input from P.D.W and T.H.A.F. All authors contributed to writing the manuscript. The authors discussed the results with each other at all stages.

Author information

The authors declare no competing financial interests. Correspondence and requests for materials should be addressed to P.D.W. (p.d.williams@reading.ac.uk).

Figure 1: Annual-mean temperature trends in the North Atlantic at 250 hPa over the period 1979–2017. Linear trends are calculated using ordinary least-squares regression from the (a) ERA-Interim, (b) NCEP/NCAR, and (c) JRA-55 reanalysis datasets. Significant ($p < 0.05$; $n = 39$) trends are indicated by stippling.

Figure 2: Vertical profiles of trends in the annual-mean north–south temperature difference across the North Atlantic over the period 1979–2017. Linear trends are calculated from the (a) ERA-Interim, (b) NCEP/NCAR, and (c) JRA-55 reanalysis datasets. Red and blue shading represents positive and negative trends, respectively. Error bars represent the 95% confidence intervals in the slope of the ordinary least-squares regression ($n = 39$).

Figure 3: Time series of annual-mean wind characteristics in the North Atlantic at 250 hPa over the period 1979–2017. Panel (a) shows the vertical shear in the zonal wind,

and panel (b) shows the zonal wind speed. Data are presented from the ERA-Interim, NCEP/NCAR, and JRA-55 reanalysis datasets. Also shown are the mean of the three reanalysis datasets and the linear trend in the mean.

Figure 4: Annual-mean trends in vertical shear in zonal wind in the North Atlantic at 250 hPa over the period 1979–2017. Panels (a), (b), and (c) show the actual vertical wind shear trends calculated from the wind field, whereas panels (d), (e), and (f) show the expected vertical wind shear trends calculated from the temperature field using thermal wind balance. Linear trends are calculated using ordinary least-squares regression from the (a, d) ERA-Interim, (b, e) NCEP/NCAR, and (c, f) JRA-55 reanalysis datasets. Significant ($p < 0.05$; $n = 39$) trends are indicated by stippling. To indicate the climatological jet stream position, the 1979–2017 annual-mean zonal wind at 250 hPa in each reanalysis dataset is also shown (black contours every 5 m s^{-1}).

Methods

The North Atlantic region was chosen partly because it is the world's busiest oceanic flight corridor. Due to the zonally extended nature of the polar jet stream in this region, transatlantic flights are typically affected by the strength and position of the jet stream throughout their entire flight paths. The effects of the jet stream on aircraft include headwinds, tailwinds, and clear-air turbulence. A further reason for choosing the North Atlantic is that – unlike the North Pacific – it exhibits separate polar and subtropical jet streams, allowing an analysis of the polar jet stream exclusively.

We used pressure-level zonal wind and temperature data from the ERA-Interim, NCEP/NCAR, and JRA-55 reanalysis datasets at six-hourly analysis intervals from 1 January 1979 to 31 December 2017 inclusive, giving 39 full years of data. All datasets were used on a standard latitude–longitude grid (0.75° for ERA-Interim, 2.5° for NCEP/NCAR, and 1.25°

for JRA-55). Trends were calculated using ordinary least-squares regression, and statistical significance was assessed at the 95% confidence level ($p < 0.05$) according to a two-tailed *t*-test. The effect of temporal autocorrelation on statistical significance was tested in the computed annual-mean data and found to be negligible. Percentage changes were calculated using the values of the fitted linear trend lines in 1979 and 2017.

To calculate the two-box zonal-mean bulk meridional temperature difference, we first averaged the annual-mean temperature in a subtropical box (30–50°N, 10–80°W) and a polar box (50–70°N, 10–80°W), with a cosine(latitude) weighting factor to account for the convergence of grid points at high latitudes. The latitudinal bounds of these boxes were chosen to be approximately either side of the climatological annual-mean jet stream latitude in the North Atlantic. We then found the meridional temperature difference across the North Atlantic by subtracting the subtropical box temperature from the polar box temperature.

The jet stream was analysed in the North Atlantic region (10–80°W, 30–70°N). The annual-mean regional-mean 250 hPa vertical shear in zonal wind was calculated by taking a centred vertical finite difference using the annual-mean zonal winds at 300 and 200 hPa:

$$-\left.\frac{\partial u}{\partial p}\right|_{250\ \mathrm{hPa}} \approx \frac{u(200\ \mathrm{hPa}) - u(300\ \mathrm{hPa})}{100\ \mathrm{hPa}}\ . \qquad (3)$$

We also calculated trends in the annual-mean regional-mean (area-weighted) zonal wind speed at 250 hPa over the North Atlantic region. Vertical profiles of vertical shear trends were calculated by taking centred finite differences at 50 hPa intervals for ERA-Interim and JRA-55, and from neighbouring pressure levels in NCEP/NCAR (due to the spacing of available pressure-level data).

The annual-mean regional-maximum vertical shear was calculated by a similar centred-difference method: we first subtracted the 300 hPa zonal wind from the 200 hPa zonal wind and then found the maximum value within the North Atlantic region at each six-hourly interval, before averaging the maximum values annually. For the annual-mean regional-maximum zonal wind speed, we found the maximum 250 hPa zonal wind speed within the North Atlantic region at each six-hourly interval, before averaging annually. In both cases, the latitude at which the maximum occurred was stored.

When the calculations in **Figure 3** are repeated using the annual-mean regional-maximum vertical shear, instead of the annual-mean regional-mean vertical shear, a significant ensemble-mean increase of 11% ($p < 0.01$) in the shear is found. The individual increases are 10% in ERA-Interim ($p < 0.01$), 18% in NCEP/NCAR ($p < 0.01$), and 7% in JRA-55 ($p < 0.01$) (**Extended Data Figure 2**). These results confirm that the shear is strengthening within the jet core as well as throughout the broader region influenced by the jet stream. The trends are not attributable to a shift in the annual-mean latitude of the jet core, which shows no significant trend over the period (**Extended Data Figure 3**).

We used the time derivative of the thermal wind balance equation to relate linear trends in the meridional temperature gradient to linear trends in the vertical wind shear. At 250 hPa, we calculated trends in the annual-mean values of $\partial u/\partial p$ (using the centred finite difference method outlined above) and $\partial T/\partial y$. The agreement between the two was assessed through Pearson's correlation coefficient using an area-weighted pattern correlation.

According to thermal wind balance, the trend in the zonal wind speed in the upper troposphere and lower stratosphere is given by the vertical integral of equation (2). This vertical integral is performed throughout the depth of the free troposphere, starting from the top of the planetary boundary layer. Temperature gradients in the lower troposphere are

included in the integral, and therefore Arctic amplification at low levels is able to influence the wind speed at upper levels. For example, written in equation form, we have:

$$\frac{\partial u(250\ \mathrm{hPa})}{\partial t} = \int_{p_0}^{450\ \mathrm{hPa}} \frac{R}{fp}\frac{\partial}{\partial t}\left(\frac{\partial T}{\partial y}\right) dp + \int_{450\ \mathrm{hPa}}^{250\ \mathrm{hPa}} \frac{R}{fp}\frac{\partial}{\partial t}\left(\frac{\partial T}{\partial y}\right) dp \approx 0\,, \qquad (4)$$

where p_0 is the pressure at the top of the planetary boundary layer. Here, the free troposphere has been divided into two layers at 450 hPa, by reference to **Figure 2**. The lower boundary term $\partial u(p_0)/\partial t$ arising from the vertical integration has been neglected in equation (4), because the trend in zonal wind speed in the lower troposphere is not significantly different from zero in any of the reanalysis datasets, as shown in **Extended Data Figure 1 (d, e, f)**. Our study shows that, on the right-hand side of equation (4), the first integral (which includes the weakening low-level temperature gradient from Arctic amplification) and the second integral (which includes the strengthening upper-level temperature gradient) are essentially equal and opposite when averaged over the North Atlantic region, thus largely cancelling out and leaving no significant trend in the upper-level speed.

Data availability statement

The NCEP/NCAR reanalysis data may be obtained from the National Oceanic and Atmospheric Administration (NOAA) Oceanic and Atmospheric Research (OAR) Earth System Research Laboratory (ESRL) Physical Sciences Division (PSD), Boulder, Colorado, USA (https://www.esrl.noaa.gov/psd/). The ERA-Interim and JRA-55 reanalysis data may be obtained from the Research Data Archive at the National Center for Atmospheric Research (NCAR), Computational and Information Systems Laboratory, Boulder, Colorado, USA (https://doi.org/10.5065/D6CR5RD9 and https://doi.org/10.5065/D6HH6H41, respectively).

Code availability statement

The analytical computer codes are publicly available at http://doi.org/10.5281/zenodo.3238842.

Extended Data Figure 1: Vertical profiles of annual-mean trends in wind characteristics in the North Atlantic over the period 1979–2017. Panels (a, b, c) show trends in the vertical shear in the zonal wind, and panels (d, e, f) show trends in the zonal wind speed. Linear trends are calculated from the (a, d) ERA-Interim, (b, e) NCEP/NCAR, and (c, f) JRA-55 reanalysis datasets. Red and blue shading represents positive and negative trends, respectively. Error bars represent the 95% confidence intervals in the slope of the ordinary least-squares regression (n = 39).

Extended Data Figure 2: Annual-mean regional-maximum six-hourly vertical shear in zonal wind in the North Atlantic at 250 hPa over the period 1979–2017. Data are presented from the ERA-Interim, NCEP/NCAR, and JRA-55 reanalysis datasets. Also shown are the mean of the three reanalysis datasets and the linear trend in the mean.

Extended Data Figure 3: Annual-mean latitude of the core of the polar jet stream in the North Atlantic at 250 hPa over the period 1979–2017. Panel (a) shows the annual-mean latitude of the regional-maximum six-hourly vertical shear in zonal wind, and panel (b) shows the annual-mean latitude of the regional-maximum six-hourly zonal wind speed. Data are presented from the ERA-Interim, NCEP/NCAR, and JRA-55 reanalysis datasets. Also shown are the mean of the three reanalysis datasets and the linear trend in the mean, which has a statistically insignificant slope of (a) –0.1 degrees decade^{-1} (p = 0.54) and (b) 0.01 degrees decade^{-1} (p = 0.76).

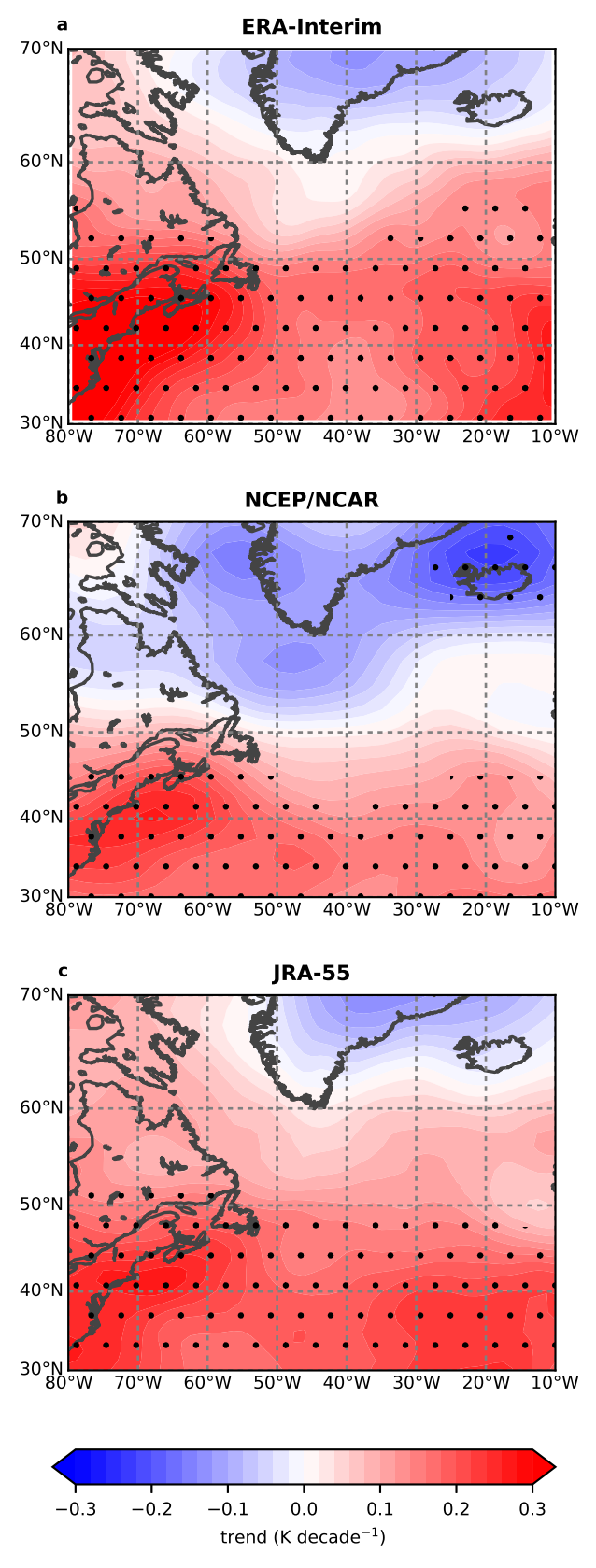
a
ERA-Interim
b
NCEP/NCAR
c
JRA-55
70°N
60°N
50°N
40°N
30°N
80°W
70°W
60°W
50°W
40°W
30°W
20°W
10°W
−0.3
−0.2
−0.1
0.0
0.1
0.2
0.3
trend (K decade^{-1})

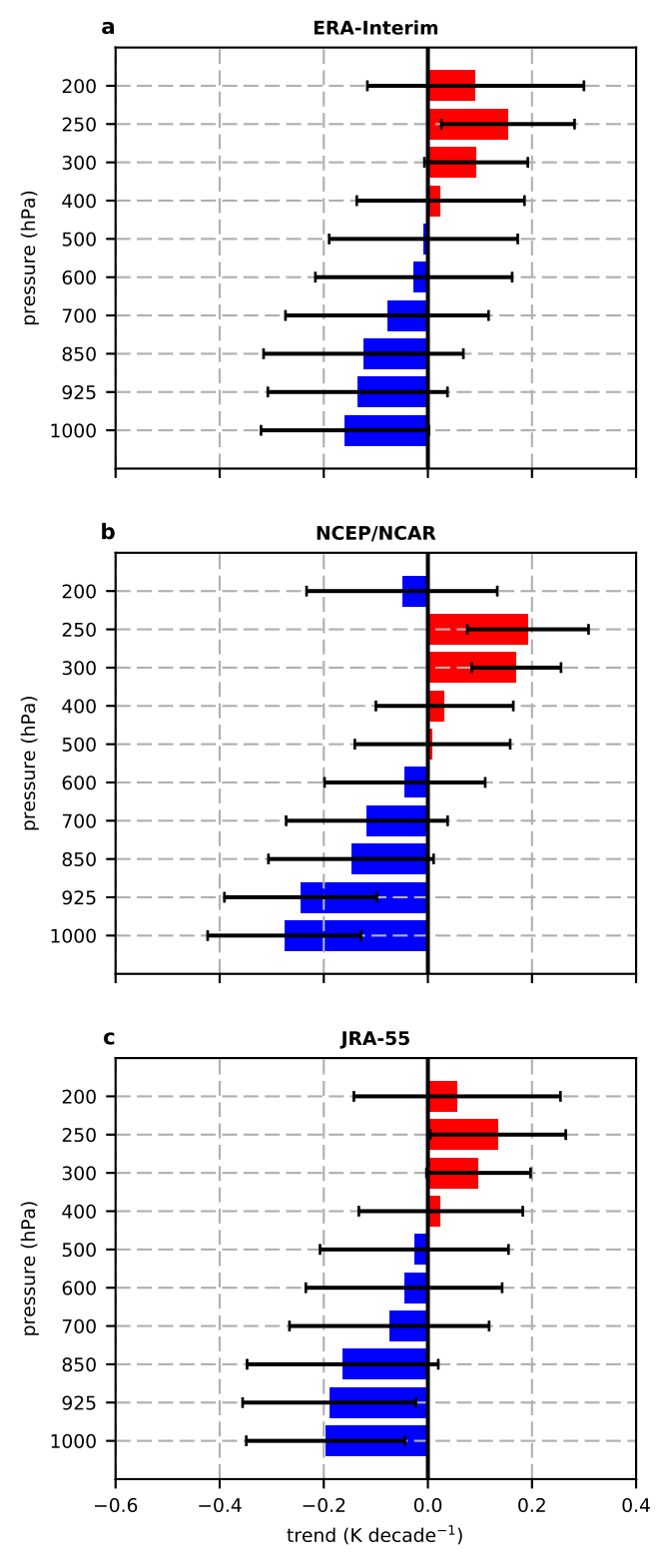
a
ERA-Interim
b
NCEP/NCAR
c
JRA-55
pressure (hPa)
200
250
300
400
500
600
700
850
925
1000
−0.6
−0.4
−0.2
0.0
0.2
0.4
trend (K decade^{-1})

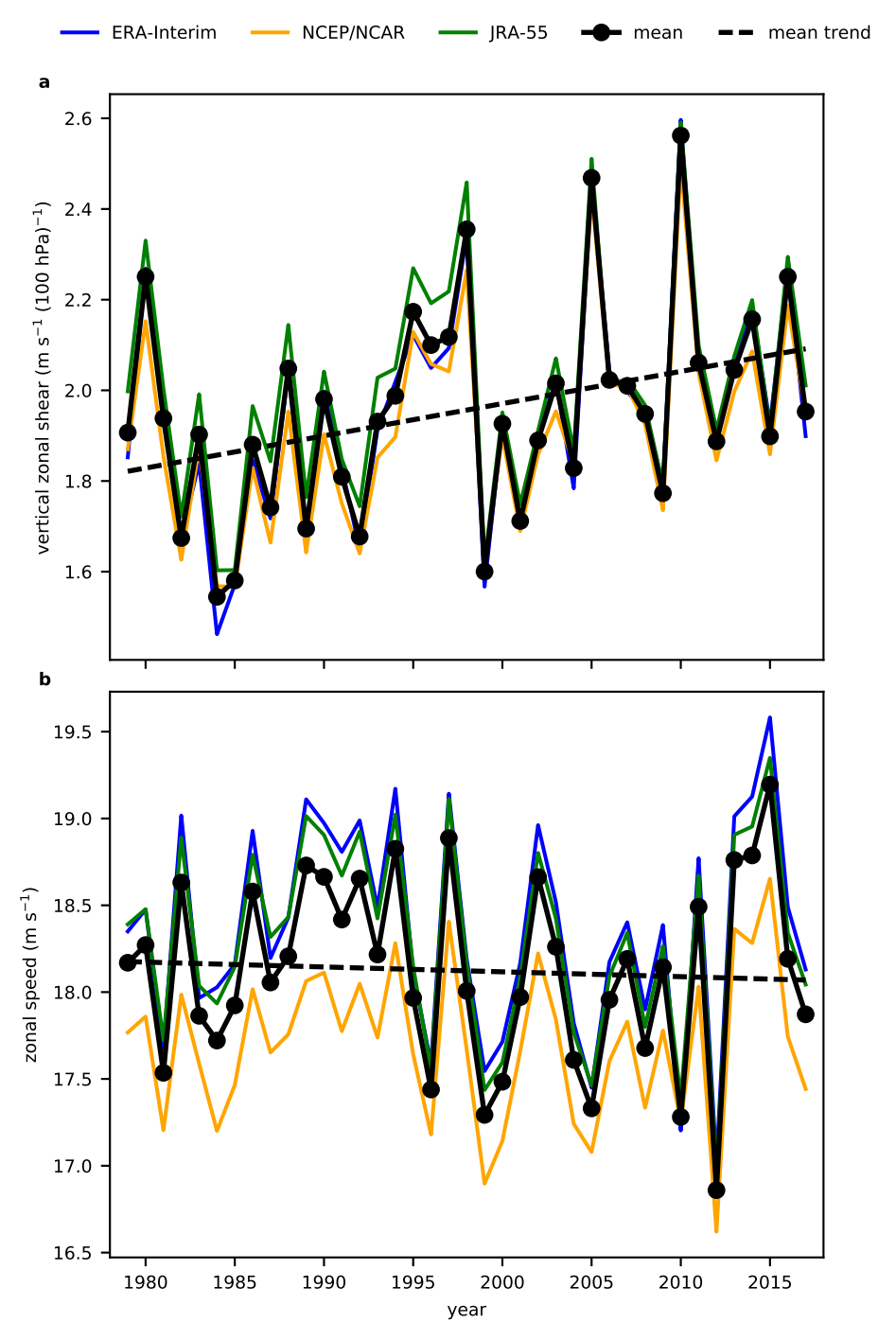
ERA-Interim
NCEP/NCAR
JRA-55
mean
mean trend
a
vertical zonal shear (m s^{-1} (100 hPa)$^{-1}$)
2.6
2.4
2.2
2.0
1.8
1.6
b
zonal speed (m s^{-1})
19.5
19.0
18.5
18.0
17.5
17.0
16.5
1980
1985
1990
1995
2000
2005
2010
2015
year

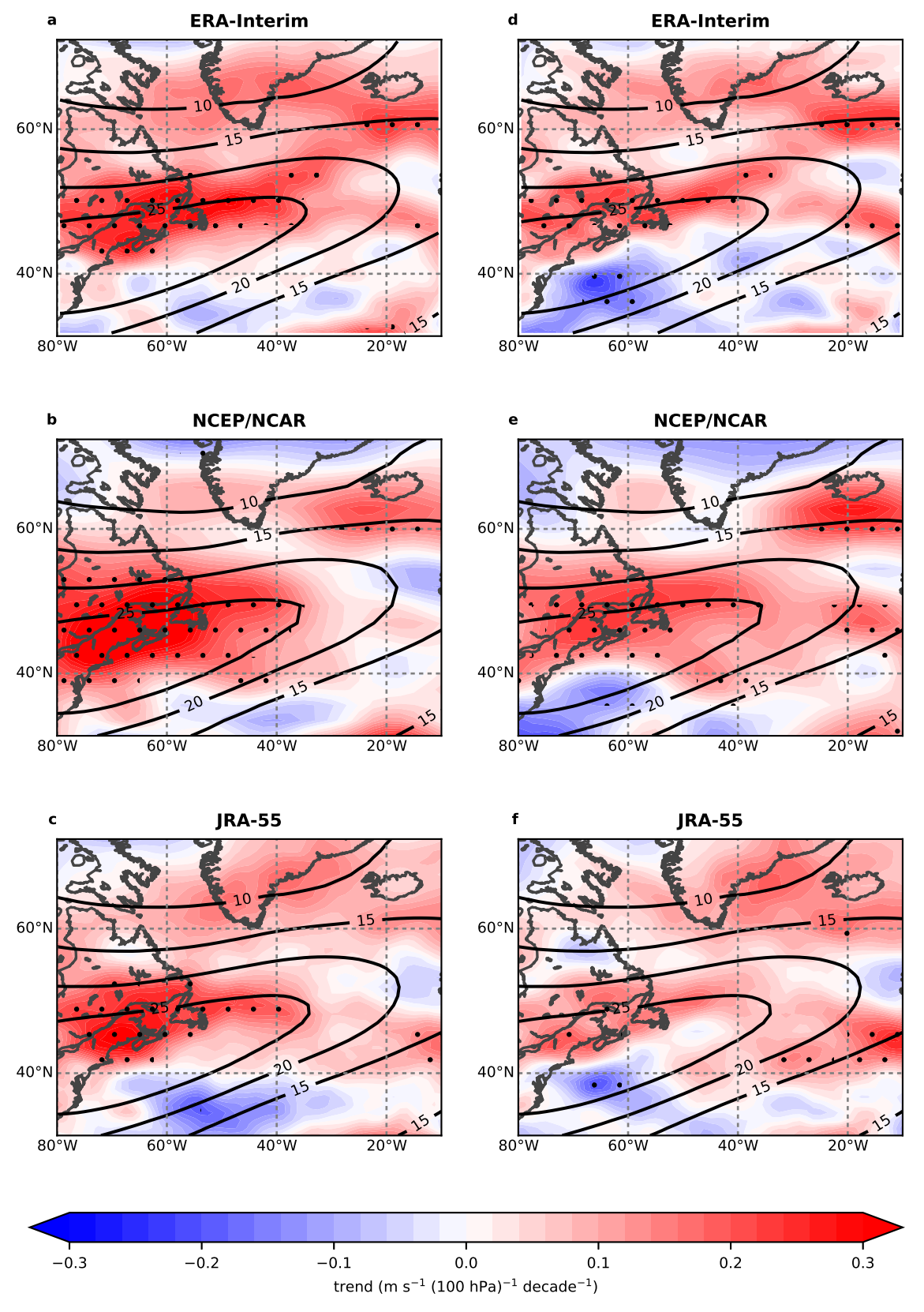
a
ERA-Interim
d
ERA-Interim
b
NCEP/NCAR
e
NCEP/NCAR
c
JRA-55
f
JRA-55
60°N
40°N
80°W
60°W
40°W
20°W
10
15
20
25
−0.3
−0.2
−0.1
0.0
0.1
0.2
0.3
trend (m s^{-1} (100 hPa)$^{-1}$ decade^{-1})